CHEMISTRY
A EUROPEAN JOURNAL

ChemPubSoc
Europe

DOI: 10.1002/chem.201300793

Host–Guest Complexation of [60]Fullerenes and Porphyrins Enabled by "Click Chemistry"

Khanh-Hy Le Ho,[a] Ismail Hijazi,[a] Lucie Rivier,[a] Christelle Gautier,[a] Bruno Jousselme,[b] Gustavo de Miguel,[c] Carlos Romero-Nieto,[c] Dirk M. Guldi,[c] Benoit Heinrich,[d] Bertrand Donnio,[d] and Stéphane Campidelli*[a]

Dedicated to Professor Maurizio Prato on the occasion of his C60th birthday

Abstract: Herein the synthesis, characterization, and organization of a first-generation dendritic fulleropyrrolidine bearing two pending porphyrins are reported. Both the dendron and the fullerene derivatives were synthesized by Cu^{I}-catalyzed alkyne–azide cycloaddition (CuAAC). The electron-donor–acceptor conjugate possesses a shape that allows the formation of supramolecular complexes by encapsulation of C_{60} within the jaws of the two porphyrins of another molecule. The interactions between the two photoactive units (i.e., C_{60} and Zn–porphyrin) were confirmed by cyclic voltammetry as well as by steady-state and time-resolved spectroscopy. For example, a shift of about 85 mV was found for the first reduction of C_{60} in the electron-donor–acceptor conjugate compared with the parent molecules, which indicates that C_{60} is included in the jaws of the porphyrin. The fulleropyrrolidine compound exhibits a rich polymorphism, which was corroborated by AFM and SEM. In particular, it was found to form supramolecular fibrils when deposited on substrates. The morphology of the fibrils suggests that they are formed by several rows of fullerene–porphyrin complexes.

Keywords: charge transfer · click chemistry · fullerenes · porphyrinoids · supramolecular chemistry

Introduction

Fullerene-based supramolecular assemblies have been extensively investigated in the last 15 years. The early work was mainly concerned with the complexation of C_{60} with molecular building blocks that favor the formation of inclusion complexes.[1] Later, more sophisticated structures, in which the encoding information was introduced onto fullerene by using classical covalent functionalization, were reported. This approach has permitted the size, order, and complexity of the supramolecular assemblies to be continuously increased and has led to, for example, fullerene-based micelles, vesicles, and aggregates,[2–10] polymers,[11–17] and liquid crystals,[18–27] as well as the organization of fullerene on electrode or nanoparticle surfaces.[28–30]

The interest in fullerene-based materials stems from the remarkable properties of C_{60}, such as its electron-accepting nature and the low re-organization energy in electron transfer. With the aim of achieving efficient electron and/or energy transfer, a wide variety of electron donors have been associated with C_{60}. In particular, combining porphyrins with C_{60} has evolved as a powerful strategy for the synthesis of mimics of natural photosynthetic systems and active materials for photovoltaic applications.[28,29,31,32] Porphyrins, and in particular face-to-face bis-porphyrin systems, are known to form host–guest complexes with C_{60} that spontaneously lead to discrete supramolecular assemblies[33–42] or polymers/arrays of interleaved porphyrins and fullerenes.[43–48] The aim of this work was the covalent linkage of jaw-like porphyrin building blocks to fullerenes to create a key–receptor self-assembly and allow the formation of self-assembled head-to-tail polymers by the intermolecular complexation of C_{60} within the jaws of the bis-porphyrin construct. Among the impressive literature on fullerenes and porphyrins, many examples of the synthesis of fullerene/porphyrin covalent dyads have been reported;[32,49–53] however, to the best of our knowledge, a molecular key–receptor for supramolecular assembly purposes has not been investigated. Note

[a] Dr. K.-H. L. Ho, Dr. I. Hijazi, L. Rivier, Dr. C. Gautier, Dr. S. Campidelli
IRAMIS, Laboratoire d'Electronique Moléculaire
SPEC (URA 2464), CEA-Saclay, 91191 Gif-sur-Yvette (France)
Fax: (+33) 1-69-08-66-40
E-mail: stephane.campidelli@cea.fr

[b] Dr. B. Jousselme
IRAMIS, Laboratoire de Chimie des Surfaces et Interfaces, SPCSI
CEA-Saclay, 91191 Gif-sur-Yvette (France)

[c] Dr. G. de Miguel, Dr. C. Romero-Nieto, Prof. D. M. Guldi
Department of Chemistry and Pharmacy
and Interdisciplinary Center of Molecular Materials
Friedrich-Alexander-Universität Erlangen-Nürnberg
Egerlandstrasse 3, 91058 Erlangen (Germany)

[d] Dr. B. Heinrich, Dr. B. Donnio
IPCMS - UMR 7504 (CNRS/Université de Strasbourg)
23, rue du Loess, BP 43, 67034 Strasbourg CEDEX 2 (France)

Supporting information for this article is available on the WWW under http://dx.doi.org/10.1002/chem.201300793.

though, Martín and co-workers recently reported the formation of polymers and dendrimers by using this concept by combining C_{60} with dendrons bearing two or four extended tetrathiafulvalenes (exTTF).[12,13]

Herein we report the synthesis, characterization, and organization of a first-generation dendritic fulleropyrrolidine bearing two pendant porphyrins (**2**). Both the dendron and the fullerene derivative were synthesized by the Cu^{I}-catalyzed alkyne–azide cycloaddition (CuAAC) reaction,[54,55] one of the most powerful reactions in "click chemistry".[56] We also report on the synthesis of the linear fulleropyrrolidine–porphyrin **1** and porphyrin **3**, which were designed as references for optical and electrochemical studies.

Results and Discussion

The syntheses of C_{60}–ZnPs **1** and **2** and porphyrin **3**[57] are depicted in Scheme 1. Fulleropyrrolidine derivative **4** was synthesized by treating 4-(2-trimethylsilylethynyl)benzaldehyde and *N*-methylglycine with C_{60} in a 1,3-dipolar cycloaddition reaction.[58] The acetylene moiety was deprotected just before the CuAAC. Porphyrin **5** and dendron **6** were synthesized according to literature procedures.[59] Fullerene derivatives **1** and **2** were obtained by the reaction of fulleropyrrolidine **4** with **5** and **6**, respectively, and porphyrin **3** by the reaction of **5** with phenylacetylene.

The electrochemical and photophysical properties of **1** and **2** were fully characterized by cyclic voltammetry (CV) and spectroscopy, including steady-state absorption and emission spectroscopy, NMR spectroscopy, femtosecond transient absorption spectroscopy, and nanosecond flash photolysis. Moreover, the supramolecular organization of **2** was investigated by small-angle X-ray scattering, and atomic force and scanning electron microscopy.

Figure 1a shows the cyclic voltammograms of **1**–**4** in THF, and the oxidation and reduction potentials are reported in Table 1. In the positive potential region, **3** gives rise to two reversible one-electron oxidations, which have been attributed to the sequential oxidation of ZnP. In the negative potential region, no discernible reduction was observed. In contrast, **4** exhibited no signal in the oxidative region, whereas two reversible reductions corresponding to the sequential reduction of C_{60} were observed in the negative potential region. Compounds **1** and **2** both showed two reversible oxidations and two reversible reductions in the potential range of 0.8 to −1.65 V. In fact, comparison of the integrations of the oxidation signals of **1** and **2** corroborates the overall C_{60}/ZnP stoichiometries, that is, ratios of 1:1 and 1:2, respectively (see Figure S1 in the Supporting Information).

The redox potentials of **1** are similar to those of references **3** and **4**, which suggests the absence of intra- or intermolecular interactions between ZnP and C_{60} in solution. Different behavior was observed for **2**. In this case, the first oxidation and the first reduction were cathodically shifted by about 25 and 85 mV, respectively, compared with the corresponding references. Such changes have been rationalized on the basis of π–π-interacting C_{60} and porphyrins.[60,61] This interaction impacts the highest-occupied molecular orbital (HOMO) of ZnP and, in turn, facilitates its oxidation. Likewise, cathodic shifts of the first reduction of C_{60} have been observed upon encapsulation.[36] CV showed that

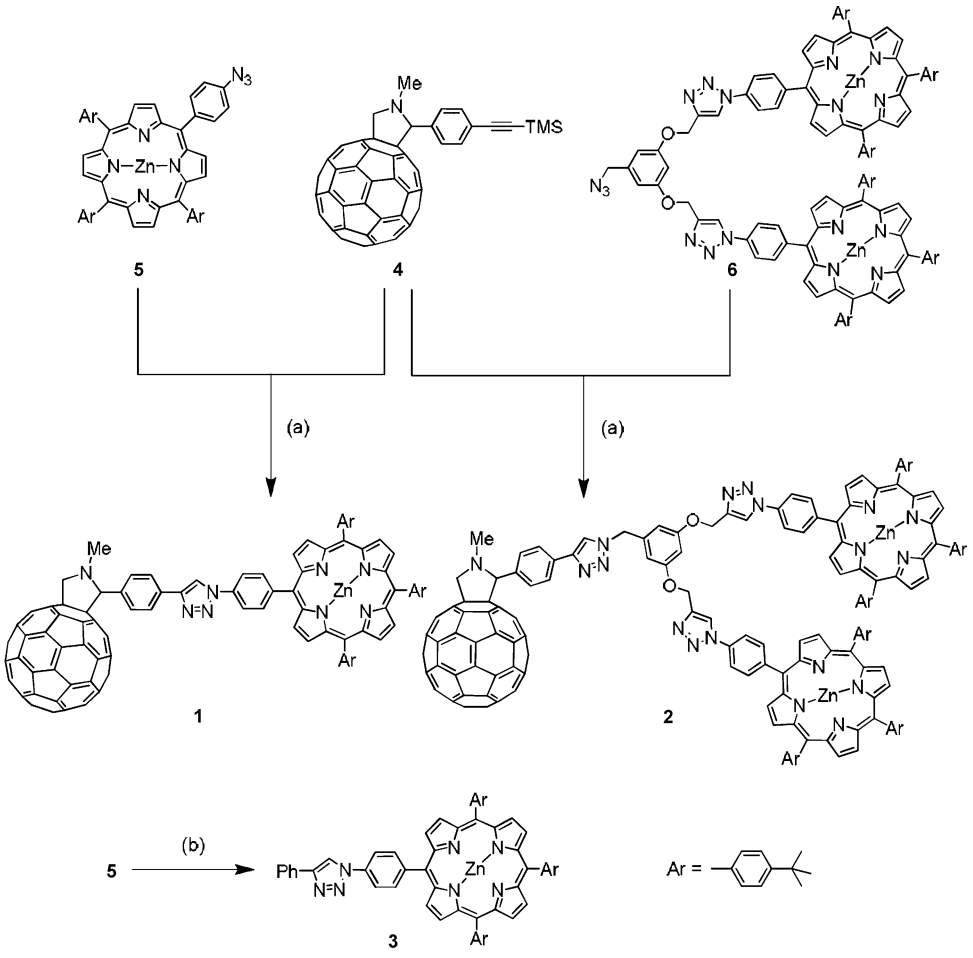

Scheme 1. Reagents and conditions: a) NBu_4F, THF, 0 °C, 1 h, then $Cu(MeCN)_4PF_6$, 2,6-lutidine, THF/H_2O, RT, for **1**: 3 days, 54%; for **2**: 4 days, 65%; b) phenylacetylene, $Cu(MeCN)_4PF_6$, 2,6-lutidine, THF/H_2O, 60 °C, 20 h, 60%.

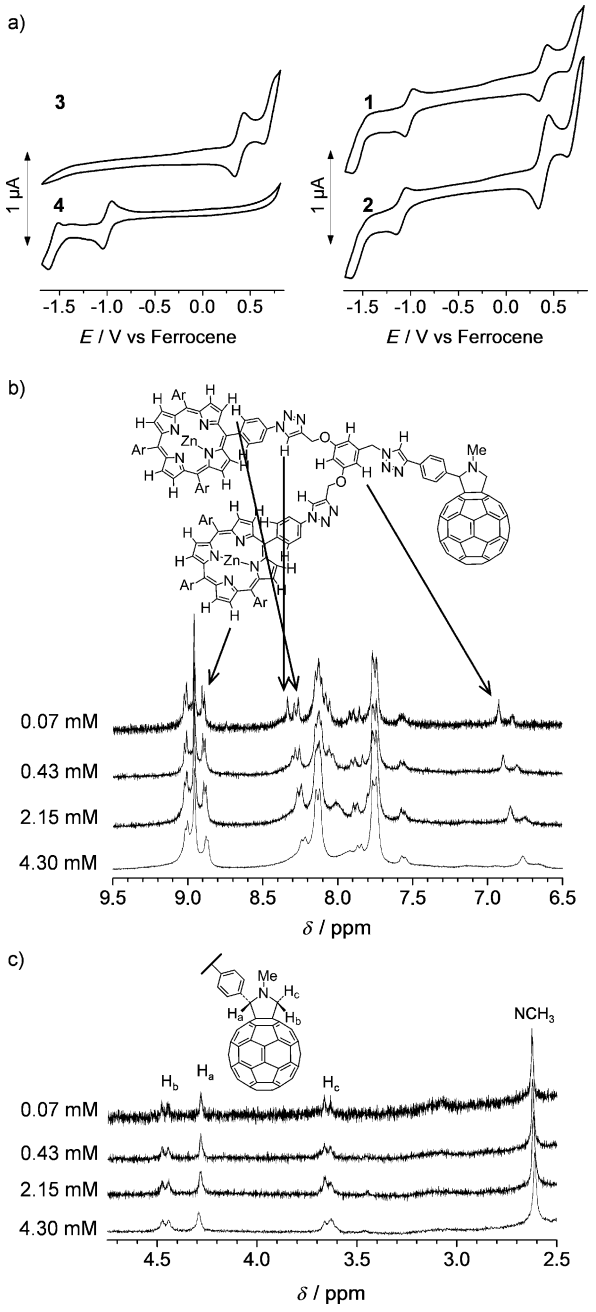

Figure 1. a) CV spectra of **1**–**4** at 10^{-3} M in 0.1 M Bu_4NPF_6/THF at 100 mV s^{-1} recorded with a platinum working electrode ($S=0.2$ mm^2); potentials determined versus ferrocene. b) Aromatic part of the ^{1}H NMR spectra of **2** and c) ^{1}H NMR spectral region showing the fulleropyrrolidine protons of **2**. The spectra were recorded at 328 K at different concentrations.

Table 1. Electrochemical potentials of ZnP **3** and C_{60} **4** as well as C_{60}–ZnP **1** and **2** in 0.1 M Bu_4NPF_6/THF with a platinum working electrode (potentials are given vs. Fc^+/Fc).

	$E^{o\prime}_{red(2)}$ [mV]	$E^{o\prime}_{red(1)}$ [mV]	$E^{o\prime}_{ox(1)}$ [mV]	$E^{o\prime}_{ox(2)}$ [mV]
3	–	–	385	705
4	−1565	−995	–	–
1	−1560	−1010	385	705
2	−1555	−1080	360	715

C_{60} is less susceptible towards reduction when it interacts with the ZnP dendrons. The second oxidation and reduction were, however, not subject to any appreciable changes due to the loss of π–π interactions in the reduced and/or oxidized form.

The ^{1}H NMR spectra of **2** recorded in 1,1,2,2-tetrachloro-[D_2]ethane at different concentrations and different temperatures are shown in Figure 1b,c and Figure S2 in the Supporting Information. The protons of the fulleropyrrolidine are less affected than the aromatic protons by an increase in concentration. In the aromatic region, the spectra show partial coalescence and an upfield shift of 0.03 to 0.20 ppm for the signals of the β-pyrrole and *meso*-phenyl protons as well as the protons of the triazole and benzyl dendron core as the concentration is increased. This behavior is likely due to the formation of large aggregates in solution rather than to the insertion of the fullerene moiety between the porphyrin jaws. Indeed, even at low concentration (ca. 10^{-5} M), the Soret band of the porphyrins in **2** shows the typical broadening and redshift characteristic of the complexation of fullerene in the porphyrin jaws.

Steady-state absorption spectroscopy was used to probe the interactions in **1** and **2** in the ground state by using three different solvents, namely toluene, THF, and benzonitrile. The absorption spectrum of **1** is best described as the sum of the individual building blocks. In contrast, the absorption spectrum of **2** shows appreciable differences compared with **1** and **3** (Figure 2a). The absorption peaks are noticeably broader and are redshifted by around 3.5 nm in toluene and by 1.5 nm in THF and benzonitrile. In addition, close inspection of the 700 nm region of the spectra in THF reveals a new absorption, which has been assigned to charge-transfer features and reflects a notable redistribution of charge density between the electron donor and the electron acceptor (see Figure S3 in the Supporting Information).[39,62] We concluded that notable electronic communication prevails in **2** between the two electro- and photoactive constituents.

Fluorescence measurements shed additional light on the interactions between ZnP and C_{60} in the excited state. After excitation at 425 nm, the fluorescence patterns of **1** and **2** match that of ZnP with maxima at 600 and 650 nm. The fluorescence quantum yields differ, however, markedly in toluene ($\Phi=0.004$ for **2**, $\Phi=0.008$ for **1**, and $\Phi=0.04$ for **3**), a trend that has tentatively been assigned to charge-transfer quenching. Further evidence for this assignment has come from the lack of notable C_{60} fluorescence in the red region, at least for **2**, which would have been indicative of an energy-transfer product. For **2**, the strong charge-transfer-induced quenching is accompanied by additional emission features in a range in which neither ZnP nor C_{60} emit appreciably. In toluene, the maximum of the new emission is at 945 nm (Figure 2b). Comparison with the ground-state absorption suggests charge-transfer character.[39,62] The quantum yield of this newly developing emission band depends on the solvent polarity, the yields decreasing in more polar environments. Moreover, the effect of temperature is quite interesting. In fact, gradually raising the temperature from

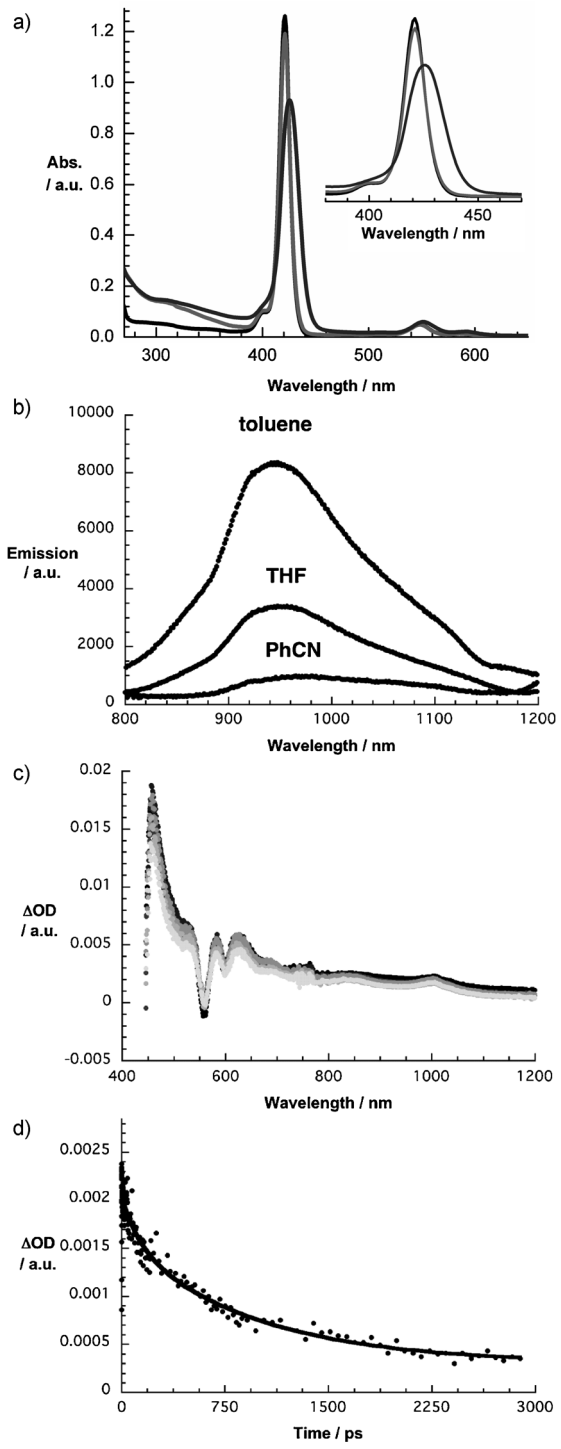

Figure 2. a) Absorption spectra of **3** (black), **1** (light grey), and **2** (dark grey) in toluene. b) Charge-transfer emission of **2** in toluene, THF, and benzonitrile (PhCN) recorded at an excitation wavelength of 425 nm. c) Differential absorption spectra (visible and near-IR) recorded upon femtosecond flash photolysis (420 nm; 110 mJ) of **2** in THF after several time delays between 0 and 125 ps at room temperature. The evolution of time is shown by the curves of black to dark grey to light grey. d) Time–absorption profile of the transient spectra in c) at 1010 nm, monitoring the charge separation and charge recombination.

25 to 75 °C leads to a deactivation of the charge-transfer emission at 945 nm and a reactivation of the intrinsic fluorescence of ZnP at 600 and 650 nm (see Figure S4 in the Supporting Information). Excess vibrational energy is thought to interrupt the charge transfer in ZnP and C_{60}. The same effects were realized when adding DABCO to **2** to coordinate the zinc center (not shown). In addition to the aforementioned changes in emission, the Soret band undergoes a significant narrowing, again an indication of diminishing ZnP–C_{60} interactions.

Next, we looked for evidence of the charge transfer by means of transient absorption measurements on the femto- and nanosecond timescales. Beginning with **3**, following the photoexcitation at 420 nm, the transient spectra exhibit typical ZnP singlet excited-state features, that is, strong maxima at 465, 575, and 630 nm as well as bleaching at 550 nm. The ZnP singlet excited state is metastable and decays slowly by intersystem crossing to the energetically lower-lying triplet excited state (see Figure S5 in the Supporting Information). Femtosecond experiments with **1** and **2** revealed again the formation of the ZnP singlet excited state upon excitation at 420 nm. But instead of seeing intersystem crossing, we observed new features corresponding to the one-electron-oxidized radical cation of ZnP, namely a broad band at around 650 nm, and the one-electron-reduced radical anion of C_{60}, a peak at 1015 nm (Figure 2c). On the nanosecond timescale, for **1**, features of the radical ion pair state are observed in THF and benzonitrile with lifetimes of 844 and 650 ns. Lifetimes that are close to a microsecond and that are solvent-dependent prompt charge-transfer dynamics driven by a through-bond mechanism. In toluene, the C_{60} triplet excited state evolves as a thermodynamically favored product of charge recombination. In contrast, the lifetime of **2** is as short as 286 ns, a finding that is rationalized on the basis of a through-space mechanism driven by intermolecular charge-transfer interactions.

In short, strong electronic communications dominate both the ground- and excited-state features in **2**. As a necessity, compact packing between the two electro- and photoactive constituents is assumed. To this end, two scenarios, intramolecular versus intermolecular complexation, are envisioned and prompted a concentration-dependent investigation starting at 10^{-10} M and reaching 10^{-5} M. However, in this range, no appreciable changes were noted in terms of absorption (i.e., position or width of the Soret and Q-bands) or emission (i.e., relative ratio between the 600/650 and 945 nm bands). There is no doubt that in this concentration range intramolecular forces govern the charge-transfer interactions. In this regard, two structural details of **2** are crucial: 1) The overall flexibility around the triazole and 2) the length of the connecting linker. Based on these observations, we postulated that **2** can fold to ensure tight intramolecular arrangements. Structures of the intramolecular complex were simulated and relaxed by using HyperChem software (MM+ method) and it appears that the C_{60} moiety can be complexed in the porphyrin jaw of the same molecule (see Figure S6 in the Supporting Information). It is only in the

10^{-4} M range that the 600/650 to 945 nm ratio changes and the 945 nm charge-transfer emission starts to take over. Accordingly, we hypothesize the commencement of intermolecular complexation in line with the AFM experiments (see below).

Complementary measurements by AFM helped to corroborate the aforementioned conclusions. Dichloromethane solutions of **2** deposited onto silicon surfaces revealed the presence of cylindrical fibrils. Two different concentrations of **2** were deposited and, in both cases, the AFM images showed similar objects on the surface. Thus, compound **2** forms fibrils with diameters of 20–25 and 2–3 nm when deposited from the more (0.40 mM) and less concentrated solutions (0.15 mM), respectively (Figure 3). In contrast, **1** did not show any nanostructures (see Figure S7 in the Supporting Information) under the same conditions. Note that below 0.15 mM the formation of fibril structures of **2** was not clearly observed.

The size of **2** was estimated by molecular modeling (Figure 3i). In particular, in the fully extended conformation **2** exhibits a conical shape with a length of 4.3 nm and a maximal height of about 1.8 nm. In this conformation, the size of the cavity allows the complexation of C_{60} from a neighboring molecule. The postulated head-to-tail organization is shown in Figure 3j. Due to the differences in the molecular dimensions of **2** and the fibrils, one can suppose that the fibrils are formed of several rows of molecules.

SEM investigations were performed on **2** and fulleropyrrolidine **4**. Our first intention was to crystallize **2**. Despite several attempts, we were unsuccessful in obtaining sufficiently large monocrystals. However, important morphological differences were observed when the crystallization was induced by the slow diffusion of acetonitrile into THF solutions of **2** or **4**. For **2**, an iridescent solution containing nanospheres of **2** evolved after 2 days. The suspension was drop-cast on to silicon wafers and imaged by SEM (Figure 4a,b). The spheres have an average diameter of around 400–500 nm and are hollow. Under the same conditions of "crystallization", **4** showed radically different behavior. In this case, nanoplates of 1–3 μm length and roughly 50–100 nm thickness were formed (Figure 4c,d). Compound **4** is likely to organize into bilayer structures in the nanoplates. In fact, similar nano-objects have been reported by Nakanishi et al. for fulleropyrrolidines containing long alkyl chains.[5,6] The supramolecular organization of **2** into hollow spheres and the role of the ZnP jaws appears to be less intuitive, but seems to be driven by its overall conical-like shape and its tendency to form long polymeric strands.

Finally, to shed light on the supramolecular organization of **2** and **4** in the nanostructures, we performed small-angle X-ray scattering on both the nanospheres and nanoplates. As expected, due to the isotropic shape and dimensions of the nanospheres, only broad and weakly intense diffusions instead of a diffraction pattern were seen for **2**. In stark contrast, the diffractograms recorded for the nanoplates formed by **4** show sharp signals with the following three sharp reflections: $d_1 = 21.675$ Å, $d_2 = 10.77$ Å, and $d_3 = 7.085$ Å (Figure 4e). These reflections, with a spacing ratio 1:2:3, indicates a long-range lamellar organization of the C_{60} moieties with an average lamellar periodicity of $d = 21.5$ Å. The presence of numerous additional, sharp and intense diffraction reflections with mixed *hkl* indices nevertheless indicates sharp boundaries and the long-range three-dimensional extension of the supramolecular nanostructure formed by **4**. The *d*-layer spacing is in good agreement with the length of

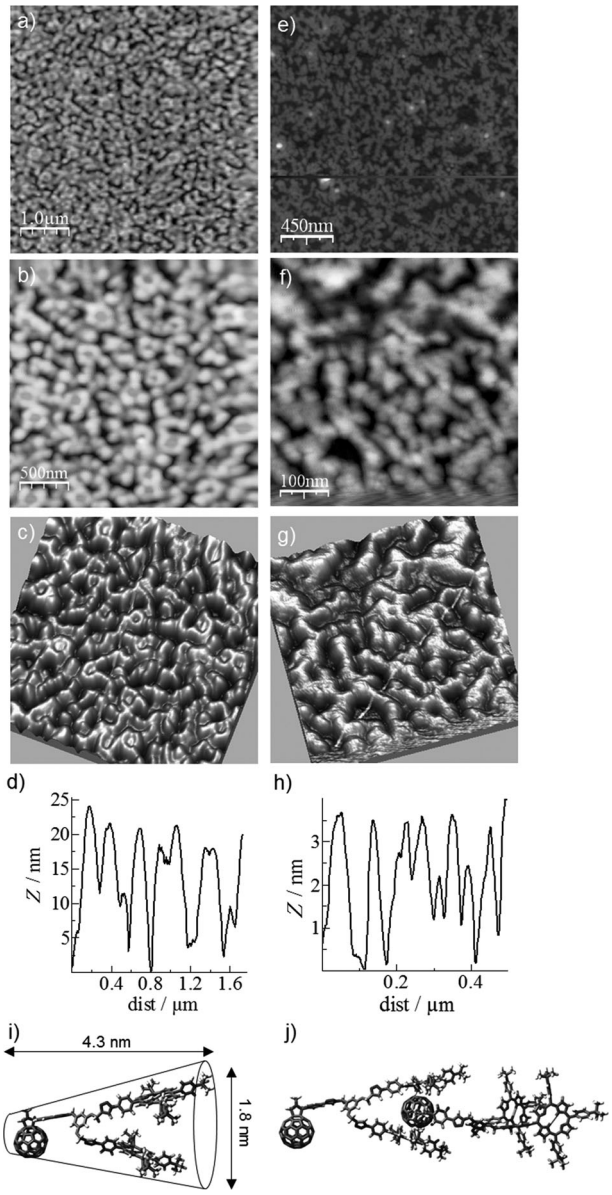

Figure 3. AFM images of **2** deposited by spin-casting on to Si/SiO_2 substrates different concentrations of **2** in dichloromethane. a,b) 0.40 mM **2**; views of the surface at different magnifications, that is, 5×5 and 2.5×2.5 μm. c) 3D topography of b). d) Profile of the AFM image showing the heights of the objects. e,f) 0.15 mM **2**; views of the surface at different magnifications, that is, 2.25×2.25 and 0.5×0.5 μm. g) 3D topography of f). h) Profile of the AFM image showing the heights of the objects. i) Representation of **2**. j) Postulated organization of molecules of **2** through complexation of C_{60} in the cone formed by the two ZnPs of a neighboring molecule.

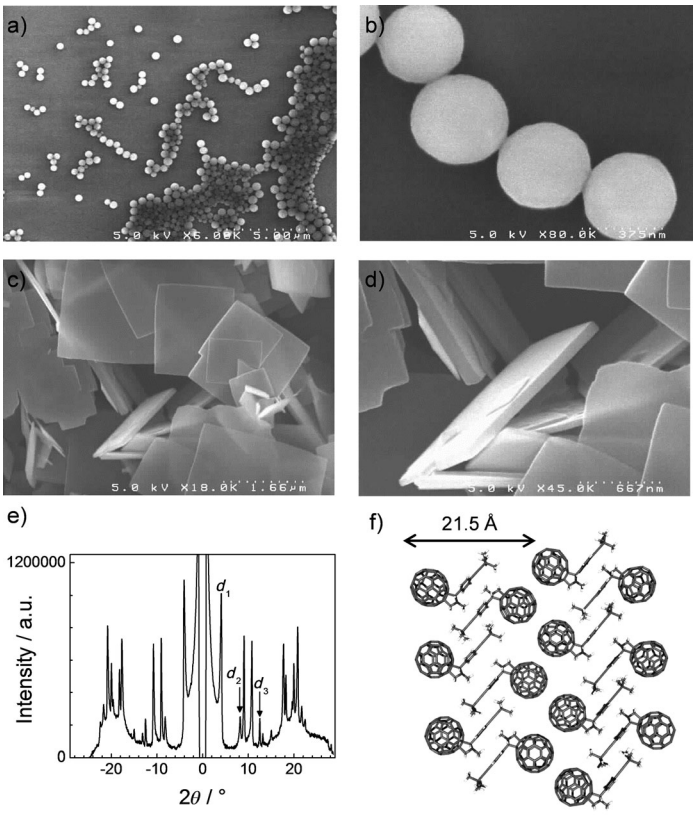

Figure 4. a,b) SEM images of aggregates of **2** deposited by drop-casting solutions of **2** in THF/ACN onto Si/SiO_2 substrates. c,d) SEM images of aggregates of fulleropyrrolidine **4** deposited by drop-casting solutions of **2** in THF/ACN onto Si/SiO_2 substrates. e) Small-angle X-ray diffractogram of the nanoplates formed by **4**. f) Postulated organization of bilayers of fulleropyrrolidines.

a fully extended conformation of a dimer of **4** (ca. 26.4 Å) and confirms a bilayer structure, provided that the molecular pairs are tilted by around 35° within the bilayer (Figure 4f).

Conclusion

We have described herein the synthesis and characterization of two fullerene–porphyrin electron-donor–acceptor conjugates. The communication between the fullerene and porphyrin units was investigated by steady-state and time-resolved spectroscopy as well as by cyclic voltammetry. We found that the two electron-donor–acceptor conjugates exhibit slightly different behavior when photoexcited: For **1**, charge-separated features with a lifetime close to 1 μs were detected, whereas for **2** the lifetime was as short as 286 ns. This difference is explained by a through-bond charge-transfer mechanism for **1** and a through-space mechanism for **2**. In fact, **2** possesses a shape that allows the formation of a supramolecular polymer by complexation of the C_{60} moiety within the jaws of two porphyrins of another molecule. The electrochemical characterization also shows differences between the two electron-donor–acceptor conjugates. For example, a shift of about 85 mV was found for the first reduction of C_{60} in **2** compared with the values for the parent molecules, which indicates that C_{60} is included in the jaws of the porphyrin. Compound **2** exhibits a rich polymorphism, which was investigated by AFM and SEM. In particular, **2** forms supramolecular fibrils; the morphology of the fibrils suggests that they are formed of several rows of fullerene–porphyrin complexes. Finally, the supramolecular organization of **2** into hollow spheres and the role of the ZnP jaws are still not clear and new investigations to understand the formation of these structures are ongoing.

Experimental Section

Techniques: Absorption spectra were recorded in quartz cuvettes on a Perkin–Elmer Lambda 900 UV-Vis-NIR or Cary5000 (Varian) spectrophotometer. Emission spectra were recorded by using a FluoroMax-3 (HORIBA) or Cary Eclipse fluorescence spectrophotometer. FTIR spectra were recorded on a Nicolet MAGMA-IR 860 spectrometer. ^{1}H NMR spectra were recorded with a Bruker AC-300 (300 MHz) spectrometer with solvent used as internal reference; MS (MALDI-TOF): spectra were recorded with a PerseptiveBiosystems Voyager DE-STR spectrometer. Molecular modeling was performed by using the HyperChem software in conjunction with the MM+ method. Cyclic voltamperometry was performed in anhydrous tetrahydrofuran solutions (THF was distilled just before use over K/benzophenone under N_2). Electrochemical-grade tetrabutylammonium hexafluorophosphate (0.1 M as supporting electrolyte) from Fluka was used without purification. Solutions were deaerated by bubbling nitrogen through them prior to each experiment, which were performed under nitrogen. Experiments were performed in a one-compartment cell equipped with a platinum working electrode ($S=0.2$ mm^2) and a platinum counter electrode. An Ag/Ag^+ (10 mM) electrode, calibrated against the ferrocene/ferricenium couple (Fc/Fc^+) before and after each experiment, was used as reference. The reference electrode was equipped with a nonaqueous double bridge to avoid possible interference with metal cations. Electrochemical experiments were carried out with an EG&G potentiostat, model 273A. For the AFM analyses, the samples were prepared by spin-coating on silicon wafers from a solution of fullerene derivatives in dichloromethane and then investigated with a Veeco Multimode Scanning Probe Microscope equipped with a Nanoscope IIIa controller. For SEM analyses, the samples were drop-cast on silicon wafers from a THF/acetonitrile suspension and then investigated with a Hitachi S4500 scanning electron microscope. Femtosecond transient absorption studies were performed with 425 nm laser pulses (1 kHz, 150 fs pulse width, ca. 100 nJ) from an amplified Ti:sapphire laser system (Clark-MXR, Inc.). Nanosecond laser flash photolysis experiments were performed with 532 nm laser pulses from a Quanta-Ray CDR Nd:YAG system (6 ns pulse width) in a front-face excitation geometry. The experiments were performed at room temperature.

Materials: C_{60} (99.9%) was purchased from MER Corporation. Chemicals were purchased form Aldrich and were used as received. Solvents were purchased form Aldrich or VWR and were used as received. For synthesis, CH_2Cl_2 (CaH_2, N_2), toluene (K/benzophenone, N_2), THF (K/benzophenone, N_2) were distilled before use. 4-(2-Trimethylsilylethynyl)-benzaldehyde,[63] azido-porphyrin **5** and porphyrin dendron **6**[59] were synthesized according to literature procedures.

Syntheses

Fulleropyrrolidine 4: C_{60} (50 mg, 0.069 mmol) was dissolved in dry toluene (50 mL) and then 4-(2-trimethylsilylethynyl)benzaldehyde (14 mg, 0.069 mmol) and *N*-methylglycine (62 mg, 0.693 mmol) were added. The mixture was stirred overnight at reflux, and evaporated to dryness. Purification of the residue by column chromatography (eluent toluene) and precipitation (dissolution in CH_2Cl_2 and precipitation by pouring the sol-

ution into MeOH) gave pure **3** (45 mg, 68% yield) as a brown powder. ^{1}H NMR (300 MHz, $CDCl_3$): δ = 7.77 (br d, J = 7.2 Hz, 2H; arom. H), 7.55 (d, J = 8.4 Hz, 2H; arom. H), 4.99 (d, J = 9.3 Hz, 1H; H pyrrolidine), 4.93 (s, 1H; H pyrrolidine), 4.26 (d, J = 9.6 Hz, 1H; H pyrrolidine), 2.79 (s, 3H; NCH_3), 0.24 ppm (s, 9H; $SiMe_3$); FTIR (KBr): $\tilde{\nu}$ = 2948, 2779, 2155, 1500, 1462, 1427, 1331, 1246, 1216, 1122, 1103, 864, 842, 758, 704, 582, 552, 526 cm^{-1}; UV/Vis (toluene): λ_{max} = 328, 432, 703 nm; MS (MALDI-TOF): *m/z* calcd for $C_{74}H_{19}NSi$: 949.13 $[M-H]^+$; found: 948.13.

Porphyrin 3: Phenylacetylene (4μL, 0.034 mmol), $[Cu(MeCN)_4]PF_6$ (3 mg, 0.008 mmol), 2,6-lutidine (100 μL), and water (1 mL) were added to a solution of porphyrin **5** (15 mg, 0.017 mmol) in THF (10 mL). The reaction mixture was frozen and the oxygen was removed by several vacuum/argon cycles. Finally, the solution was stirred at 60°C for 20 h, then water was added, and the mixture was extracted with CH_2Cl_2. The organic phase was filtered through hydrophobic filter paper (Phase Separator Whatman filter) and evaporated to dryness. Purification of the residue by column chromatography (eluent CH_2Cl_2) gave pure **3** (10 mg, 60% yield) as a purple powder. ^{1}H NMR (300 MHz, $CDCl_3$): δ = 8.04 (d, J = 4.5 Hz, 2H; arom. H), 9.00 (s, 4H; arom. H), 8.95 (d, J = 4.8 Hz, 2H; arom. H), 8.53 (s, 1H; arom. H), 8.43 (d, J = 8.4 Hz, 2H; arom. H), 8.21 (d, J = 8.4 Hz, 2H; arom. H), 8.16 (d, J = 8.1 Hz, 6H; arom. H), 8.05 (d, J = 8.4 Hz, 2H; arom. H), 7.77 (d, J = 8.4 Hz, 2H; arom. H), 7.55 (t, J = 7.5 Hz, 2H; arom. H), 7.48–7.40 (m, 1H; arom. H), 1.63 ppm (s, 27H; C-$(CH_3)_3$); FTIR (KBr): $\tilde{\nu}$ = 2958, 2901, 2865, 1525, 1492, 1461, 1394, 1362, 1338, 1267, 1205, 1109, 1070, 998, 853, 811, 796, 758, 719, 692, 582 cm^{-1}; UV/Vis (toluene): λ_{max} = 425, 550, 589 nm; MS (MALDI-TOF): *m/z* calcd for $C_{64}H_{57}N_7Zn$: 987.40 $[M]^+$; found: 987.42.

Fullerene–porphyrin 1: A 1 M TBAF solution in THF (50 μL) was added to a solution of fullerene **4** (15 mg, 0.015 mmol) in dry THF (20 mL) at 0°C under argon. The reaction was stirred for 1 h and then water was added, and the mixture was extracted with CH_2Cl_2. The organic phase was filtered through hydrophobic filter paper (Phase separator Whatman filter) and evaporated to dryness. The fulleropyrrolidine was used directly for the coupling reaction without further purification. The fullerene derivative was redispersed in THF (30 mL) and then porphyrin **5** (12 mg, 0.013 mmol), $[Cu(MeCN)_4]PF_6$ (1.5 mg, 0.004 mmol), 2,6-lutidine (50 μL), and water (1 mL) were added. The reaction mixture was frozen and the oxygen was removed by several vacuum/argon cycles. Finally, the solution was stirred at room temperature for 3 days, then water was added, and the mixture was extracted with CH_2Cl_2. The organic phase was filtered through hydrophobic filter paper (Phase separator Whatman filter) and evaporated to dryness. Purification of the residue by column chromatography (eluent first CH_2Cl_2, then CH_2Cl_2/Et_2O, 100:3) gave pure **1** (13 mg, 54% yield) as a brown-purple powder. ^{1}H NMR (300 MHz, $CDCl_3$): δ = 9.04 (d, J = 4.8 Hz, 2H; arom. H), 8.98 (s, 4H; arom. H), 8.94 (d, J = 4.5 Hz, 2H; arom. H), 8.66 (s, 1H; arom. H), 8.38 (d, J = 8.4 Hz, 2H; arom. H), 8.23 (d, J = 8.1 Hz, 2H; arom. H), 8.20–8.10 (m, 8H; arom. H), 7.97–7.85 (br s, 2H; arom. H), 7.82–7.71 (m, 6H; arom. H), 4.90 (d, J = 9.9 Hz, 1H; H pyrrolidine), 4.85 (s, 1H; H pyrrolidine), 4.17 (d, J = 9.0 Hz, 1H; H pyrrolidine), 2.86 (s, 3H; NCH_3), 1.63 ppm (s, 27H; C-$(CH_3)_3$); FTIR (KBr): $\tilde{\nu}$ = 2953, 2924, 2901, 2863, 2779, 1523, 1490, 1460, 1395, 1361, 1336, 1266, 1205, 1108, 1069, 999, 851, 810, 796, 719, 668, 575, 552, 526 cm^{-1}; UV/Vis (toluene): λ_{max} = 425, 550, 589, 708 nm; MS (MALDI-TOF): *m/z* calcd for $C_{127}H_{62}N_8Zn$: 1762.44 $[M]^+$; found: 1762.41.

Fullerene–porphyrin 2: A 1 M TBAF solution in THF (100 μL) was added to a solution of fullerene **4** (13 mg, 0.014 mmol) in dry THF (10 mL) at 0°C under argon. The reaction was stirred for 1 h, then water was added, and the mixture was extracted with CH_2Cl_2. The organic phase was filtered through hydrophobic filter paper (Phase separator Whatman filter) and evaporated to dryness. The fulleropyrrolidine was used directly for the coupling reaction without further purification. The fullerene derivative was redispersed in THF (10 mL) and then compound **6** (14 mg, 0.007 mmol), $[Cu(MeCN)_4]PF_6$ (1.5 mg, 0.004 mmol), 2,6-lutidine (50 μL), and water (1 mL) were added. The reaction mixture was frozen and the oxygen removed by several vacuum/argon cycles. Finally, the solution was stirred at room temperature for 4 days, then water was added, and the mixture was extracted with CH_2Cl_2. The organic phase was filtered through hydrophobic filter paper (Phase separator Whatman filter) and evaporated to dryness. Purification of the residue by column chromatography (eluent first CH_2Cl_2, then CH_2Cl_2/Et_2O, 100:5 to 100:8) gave pure **2** (13 mg, 65% yield) as a brown-purple powder. ^{1}H NMR (300 MHz, $C_2D_2Cl_4$, 55°C): δ = 9.04 (d, J = 4.8 Hz, 4H; arom. H), 8.98 (s, 8H; arom. H), 8.92 (d, J = 4.2 Hz, 4H; arom. H), 8.36 (s, 2H; arom. H), 8.30 (d, J = 7.5 Hz, 4H; arom. H), 8.20–8.05 (m, 16H; arom. H), 7.93 (d, J = 8.1 Hz, 2H; arom. H), 7.88 (s, 1H; arom. H), 7.82–7.72 (m, 12H; arom. H), 7.62–7.55 (br m, 2H; arom. H), 6.94 (br s, 2H; arom. H), 6.85 (br s, 1H; arom. H), 5.57 (br s, 2H; CH_2N), 4.49 (br s, 4H; CH_2O), 4.49 (d, J=9.6 Hz, 1H; H pyrrolidine), 4.31 (s, 1H; H pyrrolidine), 3.67 (d, J=9.6 Hz, 1H; H pyrrolidine), 2.65 (s, 3H; NCH_3) 1.54 ppm (s, 54H; $C(CH_3)_3$); FTIR (KBr): $\tilde{\nu}$ = 2954, 2923, 2902, 2863, 1596, 1524, 1492, 1460, 1393, 1362, 1337, 1267, 1205, 1151, 1109, 1067, 1039, 998, 852, 810, 796, 720, 668, 576 cm^{-1}; UV/Vis (toluene): λ_{max} = 428, 553, 591 nm; MS (MALDI-TOF): *m/z* calcd for $C_{196}H_{124}N_{18}O_2Zn_2$: 2888.87 $[M]^+$; found: 2888.80.

Acknowledgements

This work was supported by ANR (projects f-DNA ANR-09-NANO-005-01 and TRANCHANT-ANR 2010 BLAN 1009 4) and by the Region Ile-de-France through the framework of C'NanoIdF, the Nanoscience Competence Center of the Paris Region (projects ElecTubes and TENAPO). K.-H.L.H. and H.I. acknowledge ANR and C'NanoIdF for doctoral and postdoctoral grants. D.M.G. and C.R.N. acknowledge the Bavarian initiative "Solar Technologies Go Hybrid" and the DFG "Excellence Cluster—Engineering of Advanced Materials".

[1] F. Diederich, M. Gómez-López, *Chem. Soc. Rev.* **1999**, *28*, 263.
[2] S. Burghardt, A. Hirsch, B. Schade, K. Ludwig, C. Böttcher, *Angew. Chem.* **2005**, *117*, 3036; *Angew. Chem. Int. Ed.* **2005**, *44*, 2976.
[3] S. Zhou, C. Burger, B. Chu, M. Sawamura, N. Nagahama, M. Toganoh, U. E. Hackler, H. Isobe, E. Nakamura, *Science* **2001**, *291*, 1944.
[4] N. Nakashima, T. Ishii, M. Shirakusa, T. Nakanishi, H. Murakami, T. Sagara, *Chem. Eur. J.* **2001**, *7*, 1766.
[5] T. Nakanishi, W. Schmitt, T. Michinobu, D. G. Kurth, K. Ariga, *Chem. Commun.* **2005**, 5982.
[6] T. Nakanishi, *Chem. Commun.* **2010**, *46*, 3425.
[7] A. M. Cassell, C. L. Asplund, J. M. Tour, *Angew. Chem.* **1999**, *111*, 2565; *Angew. Chem. Int. Ed.* **1999**, *38*, 2403.
[8] V. Georgakilas, F. Pellarini, M. Prato, D. M. Guldi, M. Melle-Franco, F. Zerbetto, *Proc. Natl. Acad. Sci. USA* **2002**, *99*, 5075.
[9] Y. Hizume, K. Tashiro, R. Charvet, Y. Yamamoto, A. Saeki, S. Seki, T. Aida, *J. Am. Chem. Soc.* **2010**, *132*, 6628.
[10] R. Charvet, Y. Yamamoto, T. Sasaki, J. Kim, K. Kato, M. Takata, A. Saeki, T. Aida, *J. Am. Chem. Soc.* **2012**, *134*, 2524.
[11] F. Giacalone, N. Martín, *Chem. Rev.* **2006**, *106*, 5136.
[12] G. Fernández, E. M. Pérez, L. Sánchez, N. Martín, *Angew. Chem.* **2008**, *120*, 1110; *Angew. Chem. Int. Ed.* **2008**, *47*, 1094.
[13] G. Fernández, E. M. Pérez, L. Sánchez, N. Martín, *J. Am. Chem. Soc.* **2008**, *130*, 2410.
[14] T. Nishimura, K. Tsuchiya, S. Ohsawa, K. Maeda, E. Yashima, Y. Nakamura, J. Nishimura, *J. Am. Chem. Soc.* **2004**, *126*, 11711.
[15] T. Haino, E. Hirai, Y. Fujiwara, K. Kashihara, *Angew. Chem.* **2010**, *122*, 8071; *Angew. Chem. Int. Ed.* **2010**, *49*, 7899.
[16] C.-L. Wang, W.-B. Zhang, R. M. Van Horn, Y. Tu, X. Gong, S. Z. D. Cheng, Y. Sun, M. Tong, J. Seo, B. B. Y. Hsu, A. J. Heeger, *Adv. Mater.* **2011**, *23*, 2951.
[17] C.-L. Wang, W.-B. Zhang, H.-J. Sun, R. M. Van Horn, R. R. Kulkarni, C.-C. Tsai, C.-S. Hsu, B. Lotz, X. Gong, S. Z. D. Cheng, *Adv. Energy Mater.* **2012**, *2*, 1375.
[18] R. Deschenaux, B. Donnio, D. Guillon, *New J. Chem.* **2007**, *31*, 1064.
[19] J. Lenoble, S. Campidelli, N. Maringa, B. Donnio, D. Guillon, N. Yevlampieva, R. Deschenaux, *J. Am. Chem. Soc.* **2007**, *129*, 9941.

[20] N. Maringa, J. Lenoble, B. Donnio, D. Guillon, R. Deschenaux, *J. Mater. Chem.* **2008**, *18*, 1524.
[21] S. Campidelli, P. Bourgun, B. Guintchin, J. Furrer, H. Stoeckli-Evans, I. M. Saez, J. W. Goodby, R. Deschenaux, *J. Am. Chem. Soc.* **2010**, *132*, 3574.
[22] T. N. Y. Hoang, D. Pociecha, M. Salamonczyk, E. Gorecka, R. Deschenaux, *Soft Matter* **2011**, *7*, 4948.
[23] H. Mamlouk, B. Heinrich, C. Bourgogne, B. Donnio, D. Guillon, D. Felder-Flesch, *J. Mater. Chem.* **2007**, *17*, 2199.
[24] J. Vergara, J. Barberá, J. L. Serrano, M. B. Ros, N. Sebastián, R. de La Fuente, D. O. López, G. Fernández, L. Sánchez, N. Martín, *Angew. Chem.* **2011**, *123*, 12731; *Angew. Chem. Int. Ed.* **2011**, *50*, 12523.
[25] M. Sawamura, K. Kawai, Y. Matsuo, K. Kanie, T. Kato, E. Nakamura, *Nature* **2002**, *419*, 702.
[26] Y. Matsuo, A. Muramatsu, R. Hamasaki, N. Mizoshita, T. Kato, E. Nakamura, *J. Am. Chem. Soc.* **2004**, *126*, 432.
[27] Y. Matsuo, A. Muramatsu, Y. Kamikawa, T. Kato, E. Nakamura, *J. Am. Chem. Soc.* **2006**, *128*, 9586.
[28] H. Imahori, *Bull. Chem. Soc. Jpn.* **2007**, *80*, 621.
[29] H. Imahori, *J. Mater. Chem.* **2007**, *17*, 31.
[30] D. Bonifazi, O. Enger, F. Diederich, *Chem. Soc. Rev.* **2007**, *36*, 390.
[31] D. Gust, T. A. Moore, A. L. Moore, *Acc. Chem. Res.* **2001**, *34*, 40.
[32] D. M. Guldi, *Chem. Soc. Rev.* **2002**, *31*, 22.
[33] P. D. W. Boyd, M. C. Hodgson, C. E. F. Rickard, A. G. Oliver, L. Chaker, P. J. Brothers, A. G. Bolskar, F. S. Tham, C. A. Reed, *J. Am. Chem. Soc.* **1999**, *121*, 10487.
[34] D. Sun, F. S. Tham, C. A. Reed, L. Chaker, M. Burgess, P. D. W. Boyd, *J. Am. Chem. Soc.* **2000**, *122*, 10704.
[35] D. Sun, F. S. Tham, C. A. Reed, L. Chaker, P. D. W. Boyd, *J. Am. Chem. Soc.* **2002**, *124*, 6604.
[36] K. Tashiro, T. Aida, J.-Y. Zheng, K. Kinbara, K. Saigo, S. Sakamoto, K. Yamaguchi, *J. Am. Chem. Soc.* **1999**, *121*, 9477.
[37] K. Tashiro, T. Aida, *Chem. Soc. Rev.* **2007**, *36*, 189.
[38] H. Sato, K. Tashiro, H. Shinmori, A. Osuka, Y. Murata, K. Komatsu, T. Aida, *J. Am. Chem. Soc.* **2005**, *127*, 13086.
[39] A. Hosseini, S. Taylor, G. Accorsi, N. Armaroli, C. A. Reed, P. D. W. Boyd, *J. Am. Chem. Soc.* **2006**, *128*, 15903.
[40] M. Ayabe, A. Ikeda, Y. Kubo, M. Takeuchi, S. Shinkai, *Angew. Chem.* **2002**, *114*, 2914; *Angew. Chem. Int. Ed.* **2002**, *41*, 2790.
[41] M. Ayabe, A. Ikeda, S. Shinkai, S. Sakamoto, K. Yamaguchi, *Chem. Commun.* **2002**, 1032.
[42] Z.-Q. Wu, X.-B. Shao, C. Li, J.-L. Hou, K. Wang, X.-K. Jiang, Z.-T. Li, *J. Am. Chem. Soc.* **2005**, *127*, 17460.
[43] P. D. W. Boyd, C. A. Reed, *Acc. Chem. Res.* **2005**, *38*, 235.
[44] D. Sun, F. S. Tham, C. A. Reed, P. D. W. Boyd, *Proc. Natl. Acad. Sci. USA* **2002**, *99*, 5088.
[45] T. Yamaguchi, N. Ishii, K. Tashiro, T. Aida, *J. Am. Chem. Soc.* **2003**, *125*, 13934.
[46] T. Hasobe, K. Saito, P. V. Kamat, V. Troiani, H. Qiu, N. Solladié, K. S. Kim, J. K. Park, D. Kim, F. D'Souza, S. Fukuzumi, *J. Mater. Chem.* **2007**, *17*, 4160.
[47] L. H. Tong, J.-L. Wietor, W. Clegg, P. R. Raithby, S. I. Pascu, J. K. M. Sanders, *Chem. Eur. J.* **2008**, *14*, 3035.
[48] T. Sagawa, S. Yoshikawa, H. Imahori, *J. Phys. Chem. Lett.* **2010**, *1*, 1020.
[49] H. Imahori, T. Umeyama, K. Kurotobi, Y. Takano, *Chem. Commun.* **2012**, *48*, 4032.
[50] D. M. Guldi, C. Luo, A. Swartz, M. Scheloske, A. Hirsch, *Chem. Commun.* **2001**, 1066.
[51] J. Iehl, R. Pereira de Freitas, B. Delavaux-Nicot, J.-F. Nierengarten, *Chem. Commun.* **2008**, 2450.
[52] M. A. Fazio, O. P. Lee, D. I. Schuster, *Org. Lett.* **2008**, *10*, 4979.
[53] G. de Miguel, M. Wielopolski, D. I. Schuster, M. A. Fazio, O. P. Lee, C. K. Haley, A. L. Ortiz, L. Echegoyen, T. Clark, D. M. Guldi, *J. Am. Chem. Soc.* **2011**, *133*, 13036.
[54] C. W. Tornøe, C. Christensen, M. Meldal, *J. Org. Chem.* **2002**, *67*, 3057.
[55] V. V. Rostovtsev, L. G. Green, V. V. Fokin, K. B. Sharpless, *Angew. Chem.* **2002**, *114*, 2708; *Angew. Chem. Int. Ed.* **2002**, *41*, 2596.
[56] H. C. Kolb, M. G. Finn, K. B. Sharpless, *Angew. Chem.* **2001**, *113*, 2056; *Angew. Chem. Int. Ed.* **2001**, *40*, 2004.
[57] M. Séverac, L. Le Pleux, A. Scarpaci, E. Blart, F. Odobel, *Tetrahedron Lett.* **2007**, *48*, 6518.
[58] M. Maggini, G. Scorrano, M. Prato, *J. Am. Chem. Soc.* **1993**, *115*, 9798.
[59] T. Palacin, H. Le Khanh, B. Jousselme, P. Jégou, A. Filoramo, C. Ehli, D. M. Guldi, S. Campidelli, *J. Am. Chem. Soc.* **2009**, *131*, 15394.
[60] F. D'Souza, R. Chitta, S. Gadde, M. E. Zandler, A. L. McCarthy, A. S. D. Sandanayaka, Y. Araki, O. Ito, *Chem. Eur. J.* **2005**, *11*, 4416.
[61] F. D'Souza, R. Chitta, S. Gadde, A. L. McCarthy, P. A. Karr, M. E. Zandler, A. S. D. Sandanayaka, Y. Araki, O. Ito, *J. Phys. Chem. B* **2006**, *110*, 5905.
[62] D. M. Guldi, A. Hirsch, M. Scheloske, E. Dietel, A. Troisi, F. Zerbetto, M. Prato, *Chem. Eur. J.* **2003**, *9*, 4968.
[63] P. Wautelet, J. Le Moigne, V. Videva, P. Turek, *J. Org. Chem.* **2003**, *68*, 8025.

Received: February 28, 2013
Published online: July 5, 2013

